

Cite this: *RSC Adv.*, 2016, 6, 3259

# Sensitive and selective detection of mercury ions based on papain and 2,6-pyridinedicarboxylic acid functionalized gold nanoparticles†

Cui Lai,<sup>\*ab</sup> Lei Qin,<sup>ab</sup> Guangming Zeng,<sup>\*ab</sup> Yunguo Liu,<sup>ab</sup> Danlian Huang,<sup>ab</sup> Chen Zhang,<sup>ab</sup> Piao Xu,<sup>ab</sup> Min Cheng,<sup>ab</sup> Xiangbin Qin<sup>c</sup> and Manman Wang<sup>ab</sup>

Here we demonstrate the rational design of a sensitive and selective colorimetric method for mercury ion ( $\text{Hg}^{2+}$ ) detection by using papain and 2,6-pyridinedicarboxylic acid (PDCA) functionalized gold nanoparticles (AuNPs). Papain is a protein with seven cysteine residues and 212 amino acid residues, which can combine with  $\text{Hg}^{2+}$ , and PDCA is a chelating ligand, which has a strong affinity for  $\text{Hg}^{2+}$ . Selectivity measurements reveal that the sensor is specific for  $\text{Hg}^{2+}$  even with interference by high concentrations of other metal ions. This sensor was also used to detect  $\text{Hg}^{2+}$  ions from real samples of tap water, river water, and pond water spiked with  $\text{Hg}^{2+}$  ions, and the results showed good agreement with the found values determined by atomic fluorescence spectrometry. The absorbance ratio ( $A_{650}/A_{520}$ ) was linear with the  $\text{Hg}^{2+}$  concentration in the range of 0.01  $\mu\text{M}$  to 14  $\mu\text{M}$ . Under the optimum conditions ( $1.0 \times 10^{-7}$  M papain,  $5.0 \times 10^{-4}$  M PDCA, pH 6.0 at 30 °C), the detection limit of  $\text{Hg}^{2+}$  was as low as 9 nM, which met the maximum allowable standard of the Environmental Protection Agency (EPA) set in drinking water. In conclusion, the P-PDCA-AuNPs sensor can be used to detect the concentration of  $\text{Hg}^{2+}$  with high sensitivity and good selectivity, and it can lead to dramatically improved colorimetric sensors.

Received 4th November 2015  
Accepted 17th December 2015

DOI: 10.1039/c5ra23157d

[www.rsc.org/advances](http://www.rsc.org/advances)

## 1. Introduction

Nowadays, the development of industry is increasing rapidly. The pollution of toxic heavy metal ions in the environment is an important issue, especially in aquatic ecosystems.<sup>1–3</sup> As a very important natural element, mercury is widely used in industry, agriculture and manufacture. Due to its strong affinity with fatty tissue in animals, mercury ions tend to biomagnify and bioaccumulate more easily than other metal ions.<sup>4–6</sup> Especially, methyl mercury is extensively present in fish species, and most of its occurrence in human originates from food through the food chain.<sup>7,8</sup> Mercury ions, as an extremely stable form of inorganic mercury, cause the damage of kidneys, brain, and the nervous and endocrine systems.<sup>9,10</sup> Therefore, the detection of mercury levels in water samples is obviously significant.

To date, a series of analytical methods have been developed to detect mercury ions. These analytical methods include flame

atomic absorption spectrometry (FAAS),<sup>11</sup> atomic fluorescence spectrometry (AFS),<sup>12</sup> inductively coupled plasma mass spectrometry (ICP-MS),<sup>13</sup> inductively coupled plasma emission spectroscopy,<sup>14</sup> electrochemical methods<sup>15</sup> and fluorescent methods,<sup>16,17</sup> and so on. Although these ways can detect mercury accurately and sensitively, these methods are partly expensive, time-consuming, rely on bulky instrumentation, ungreen, and, in some cases, are intolerant to interferences. To extend the application field of detection, varieties of colorimetric methods based on functionalized gold nanoparticles (AuNPs) have been developed for the simple, rapid and on-line determination of  $\text{Hg}^{2+}$ .<sup>18–23</sup> In recent years, rapid colorimetric sensing methods have attracted more and more interests because of their simple and inexpensive construction, rapid sensing capabilities, and high sensitivity. On the other hand, the aggregation of AuNPs can cause a range of rapid color change from ruby red to deep purple, even blue due to the coupling of interparticle Surface Plasmon Resonance (SPR), with very high extinction coefficients ( $10^8$ – $10^{10}$   $\text{M}^{-1} \text{cm}^{-1}$ ).<sup>24–26</sup> Consequently, several groups had developed colorimetric sensor for the identification of mercury ions.

Colorimetric sensors based on AuNPs have been extensively used as the detection of small concentrations of heavy metal ions such as cadmium, lead, arsenic and mercury.<sup>27–33</sup> In recently, the formation of thymine- $\text{Hg}^{2+}$ -thymine (T- $\text{Hg}^{2+}$ -T) was revealed very stably, Lee *et al.*<sup>18</sup> reported method for

<sup>a</sup>College of Environmental Science and Engineering, Hunan University, Changsha 410082, Hunan, PR China. E-mail: laicui@hnu.edu.cn; zgming@hnu.edu.cn; Fax: +86-731-88823701; Tel: +86-731-88822754

<sup>b</sup>Key Laboratory of Environmental Biology and Pollution Control (Hunan University), Ministry of Education, Changsha 410082, Hunan, PR China

<sup>c</sup>School of Mathematics and Statistics, Central South University, Changsha 410075, Hunan, PR China

† Electronic supplementary information (ESI) available. See DOI: 10.1039/c5ra23157d

colorimetric detection of  $\text{Hg}^{2+}$  based on DNA-functionalized AuNPs. This method was highly selectivity and sensitivity, but the requirement of electronic heating and read-out unit for detection at elevated temperatures made this sensor costly and impractical for rapid on-site sample analysis. To overcome these challenges, Xue *et al.*<sup>34</sup> developed a colorimetric sensor system for detection of  $\text{Hg}^{2+}$  using DNA/nanoparticle conjugates. This sensor could operate within an adjustable operating temperature range, but the detection of real samples was not given. Most of aforementioned methods determining mercury used DNA functionalized AuNPs, but few of them used enzymes. Guo *et al.*<sup>35</sup> synthesized P-AuNPs through the Au-S between papain and AuNPs to detect  $\text{Hg}^{2+}$ , the interferences of  $\text{Pb}^{2+}$  and  $\text{Cu}^{2+}$  were still inevitably. Thus, a highly sensitivity and selectivity method to detect  $\text{Hg}^{2+}$  with optics is still needed.

Darbha *et al.*<sup>36</sup> developed the method for detection of  $\text{Hg}^{2+}$  using functionalized AuNPs based on the strong affinity between 2,6-pyridinedicarboxylic acid (PDCA) and  $\text{Hg}^{2+}$ . Yu *et al.*<sup>37</sup> used PDCA to improve the selectivity toward  $\text{Hg}^{2+}$ . Inspired by these studies, in this paper, we developed a rapid colorimetric sensor to detect  $\text{Hg}^{2+}$  using papain and 2,6-pyridinedicarboxylic acid (PDCA) functionalized gold nanoparticles (P-PDCA-AuNPs). In the presence of  $\text{Hg}^{2+}$ , the functionalized AuNPs aggregated through metal-ligand interactions. The PDCA ligands bound to the AuNPs species *via* Au-N bounds, which improved the selectivity towards  $\text{Hg}^{2+}$  through a cooperative effect.<sup>36</sup>  $\text{Hg}^{2+}$  could be detected by the colorimetric response of AuNPs and UV-Vis spectrophotometer, even by the naked eyes. In the real samples analysis, the results were still satisfactory. The approach allows for sensitive and selective detection of  $\text{Hg}^{2+}$ , which has potential application in real time detection.

## 2. Materials and methods

### 2.1. Materials

Chloroauric acid hydrated ( $\text{HAuCl}_4 \cdot 4\text{H}_2\text{O}$ ) and sodium citrate were purchased from Sinopharm Chemical Reagent Co., Ltd (Beijing, China). Papain, extracting from the *Carica papaya*, was purchased from Sigma-Aldrich (USA). 2,6-Pyridinedicarboxylic acid (PDCA) was obtained from J&K Scientific Ltd (Beijing, China). Mercuric nitrate was purchased from Xiya Chemical Industry Co., Ltd (Shandong, China). All the reagents were used without further purification. Other chemicals involving metal ions salts were all of analytical grade and were obtained from Damao Reagent of Tianjin (Tianjin, China). Ultrapure water (18.2  $\Omega$ , Milli-Q Millipore) was used in each experimental process. All of the solutions were prepares in Milli-Q water, and Milli-Q water was also used for further dilution.

### 2.2. Instruments

Colorimetric measurement was recorded by a UV-2007 spectrometer (Shimadzu corporation, Kyoto, Japan) to obtain the absorption spectra of reaction solution using a quartz cuvette (1 cm path length), and the transmission electron microscopy (TEM) images of AuNPs were performed on a TECNAI T20 G<sup>2</sup> electron microscope instrument operated at an accelerating

voltage of 200 kV (FEI, Netherland). The magnification of TEM is 71 000 $\times$ . The contents of  $\text{Hg}^{2+}$  in the real samples were measured using the Atomic Fluorescence Spectrometry (AFS).

### 2.3. Preparation of AuNPs

The approximately 13 nm diameter AuNPs were prepared according to reported method with a little alteration.<sup>19,38</sup> All glassware was soaked with freshly prepared 3 : 1 (v/v)  $\text{HNO}_3$ – $\text{HCl}$  (aqua regia) for 30 min, rinsed with ultrapure water, and dried for several hours before use. An aqueous solution (100 mL) containing 1 mL  $\text{HAuCl}_4$  (0.1%) was brought to boil in a conical flask (250 mL) with rapid stirring. Upon boiling, a 38.8 mM freshly prepared sodium citrate solution (10 mL) was added quickly and left to continue boiling under stirring, within this time, the color of the solution changed from light yellow, blue, purple, finally to ruby red. When the solution turned ruby red from light yellow, the resulting solution was stirred for another 15 min at room temperature. Then, stirring was stopped, and the solution was left allowed to cool to room temperature, filtered through a 0.22  $\mu\text{m}$  syringe filter. The resulting spherical AuNPs were stored at 4  $^\circ\text{C}$ . The concentration of the prepared AuNPs was about 8.48 nM according to Beer–Lambert's law with an extinction coefficient of  $2.78 \times 10^8 \text{ M}^{-1} \text{ cm}^{-1}$  at 520 nm for the 13 nm AuNPs.<sup>37,39</sup>

### 2.4. Preparation of P-PDCA-AuNPs

To detect  $\text{Hg}^{2+}$  selectively, the surface of the AuNPs was functionalized with papain and 2,6-pyridinedicarboxylic acid (PDCA). For the preparation of P-PDCA-AuNPs, solid papain was dissolved in ultrapure water to  $1.0 \times 10^{-7} \text{ M}$  and stored in the dark at  $-20 \text{ }^\circ\text{C}$  firstly. Then, 2,6-pyridinedicarboxylic acid (PDCA) was dissolved in ultrapure water to  $5.0 \times 10^{-4} \text{ M}$ . The pH of AuNPs solutions was adjusted to 6.0 by NaOH or HCl solutions. An excess amount of papain and PDCA was added to ensure the functionalizing completely. The papain solution (0.2 mL,  $1.0 \times 10^{-7} \text{ M}$ ) was added to AuNPs solutions (2 mL, 2.12 nM). The mixture was shaken for 30 min and incubated for 12 hours in the dark. The P-AuNPs were centrifuged at 12 000 rpm for 20 min. After removing the supernatants, the sediment was resuspended in ultrapure water. PDCA solution (0.2 mL,  $5 \times 10^{-4} \text{ M}$ ) was added to the prepared P-AuNPs solutions. Finally, the mixture was shaken for another 30 min and was incubated for 6 hours in the dark. The final concentration of P-PDCA-AuNPs solutions was about 2.23 nM.

### 2.5. Colorimetric detection of $\text{Hg}^{2+}$

Colorimetric detection of  $\text{Hg}^{2+}$  was used to evaluate the range of determination concentration of  $\text{Hg}^{2+}$  with the P-PDCA-AuNPs system. The pH value was adjusted to 6.0, and then a series of  $\text{Hg}^{2+}$  solutions (0.2 mL) with different concentrations (0, 0.01, 0.1, 2, 4, 6, 8, 14, 20, 50, 100, 500, 1000, 2000  $\mu\text{M}$ ) was added into the P-PDCA-AuNPs solution in a 5 mL sample bottle. After thorough shaking, the solutions were incubated at 30  $^\circ\text{C}$  for 15 min. The color change of the mixture was observed and recorded. Then the resulting solution was measured by the UV-Vis absorption spectra over the wavelength range from 200

nm to 800 nm and the absorbance values at 520 nm ( $A_{520}$ ) and 650 nm ( $A_{650}$ ) were also measured. The ratio of  $A_{650}/A_{520}$  was calculated to indicate the aggregation degree of AuNPs. During the detection process, the final concentration of P-PDCA-AuNPs was 2.23 nM. To explore the selectivity, several commonly ions were tested using the sensing systems including  $\text{Al}^{3+}$ ,  $\text{Ca}^{2+}$ ,  $\text{Cd}^{2+}$ ,  $\text{Cu}^{2+}$ ,  $\text{Fe}^{2+}$ ,  $\text{Fe}^{3+}$ ,  $\text{K}^{+}$ ,  $\text{Mg}^{2+}$ ,  $\text{Mn}^{2+}$ ,  $\text{NH}_4^{+}$ ,  $\text{Pb}^{2+}$ ,  $\text{Zn}^{2+}$  and  $\text{Na}^{+}$  ions. The concentration of these ions in the control experiments was 20 mM and carried out for 15 min at 30 °C. The concentration of  $\text{Hg}^{2+}$  was 1 mM. UV-Vis spectra of P-PDCA-AuNPs solutions were recorded 15 min after the addition of different kinds of competing ions.

## 2.6. Analysis of real samples

Analysis of real samples was used to test the applicability of P-PDCA-AuNPs in detection of  $\text{Hg}^{2+}$ . Samples of river water, tap water and pond water were collected from the Hsiang River (Changsha, China), our laboratory and Lake of Peach, respectively. Firstly, the water samples were filtered through a 0.22  $\mu\text{m}$  syringe filter. And then, the pH of the water was adjusted to 6.0. Finally, the samples were prepared by spiking with the standard solutions of  $\text{Hg}^{2+}$ . The final concentration was 5 and 10  $\mu\text{M}$ , respectively. For further verifying the application of this system, 0.01  $\mu\text{M}$  of  $\text{Hg}^{2+}$  were also added to the real samples.

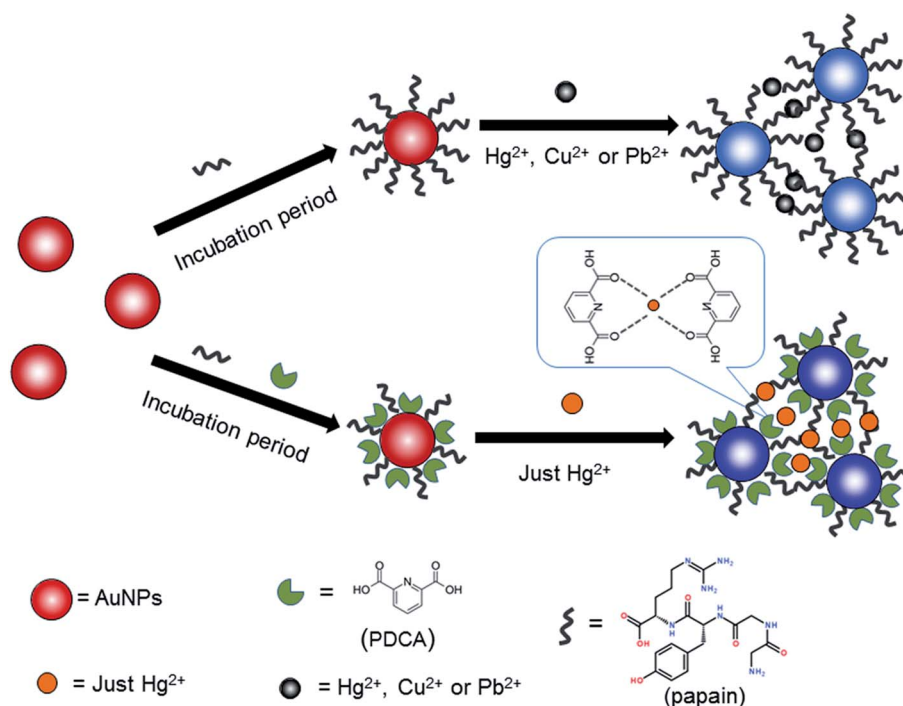
# 3. Results and discussion

## 3.1. Characterization of functionalized AuNPs

Papain, getting from the *Caria papaya*, is a plant endoprotease belonging to the cysteine endopeptidase family, which has

a single polypeptide chain including 212 amino acid residues, including seven cysteine residues, with a molecular weight of 23 400.<sup>40,41</sup> The advantages of wonderful pH span, highly sensitivity, temperature stability, low price and short response time make papain can be used for detection of  $\text{Hg}^{2+}$ .<sup>42,43</sup> Structurally, papain can coat with AuNPs on the surfaces through sulphhydryl group, and it may interact with  $\text{Hg}^{2+}$  through amino group.<sup>41</sup> Herein, papain can be used to detect  $\text{Hg}^{2+}$ . Guo *et al.*<sup>35</sup> used papain to determine  $\text{Hg}^{2+}$ , but the sensitivity and selectivity was still need to improve. Papain has seven cysteine residues, except for  $\text{Hg}^{2+}$ ,  $\text{Pb}^{2+}$  and  $\text{Cu}^{2+}$  can bind with cysteine residues. Moreover, as a protein, papain has many functional groups like other proteins, such as amino, carboxyl, hydroxyl and so on.  $\text{Pb}^{2+}$  and  $\text{Cu}^{2+}$  can interact with these groups inducing the aggregation of AuNPs. On the other hand, PDCA, as a chelating ligand, has strong affinity with  $\text{Hg}^{2+}$ .<sup>37</sup> The stability constants of heavy-metal ions with PDCA are  $\log K = 10.0$  (Cd), 8.2 (Pb), 20.2 (Hg), and 8.5 (Mn).<sup>16,44</sup> PDCA can be used as a chelating agent to achieve good selectivity because it can form much more stable complex with  $\text{Hg}^{2+}$  ions than other metal ions. Moreover, the carboxylic group of PDCA can combine with AuNPs on the surfaces. It could be used to improve the selectivity of  $\text{Hg}^{2+}$  detection (Scheme 1). As previous studies reported,<sup>37</sup> the use of PDCA as co-additive in a sensor system can improve the selectivity and sensitivity for  $\text{Hg}^{2+}$ . Thus, we suppose that if functionalized AuNPs with PDCA and papain, the level of  $\text{Hg}^{2+}$  could be determined by naked eyes and the sensitivity and selectivity also could be improved.

To demonstrate the feasibility of this assumption, the design was applied to detect  $\text{Hg}^{2+}$  using papain and PDCA functionalized AuNPs. After centrifuging, a little difference about the color



**Scheme 1** Schematic of aggregating process of P-PDCA-AuNPs induced by  $\text{Hg}^{2+}$ .

of AuNPs was observed. The UV-Vis absorption spectra of P-PDCA-AuNPs revealed broadening and slight red shift (Fig. 1). P-PDCA-AuNPs had slight polydisperse when comparing with unmodified AuNPs. It is possibly that AuNPs grew in the process of preparation. It has reported that in the citrate protected AuNPs solutions, there may exist  $\text{Au}^{3+}$  and some amino acids of papain, such as tyrosine, would reduce  $\text{Au}^{3+}$  to  $\text{Au}(0)$  in the alkaline aqueous solution. Furthermore, some reported literatures revealed that protein can reduce  $\text{Au}^{3+}$  into  $\text{Au}(0)$ .<sup>45,46</sup> Therefore, the color change indicated that papain and PDCA were modified on the surface of AuNPs. Moreover, control experiments using the papain were carried out, and 1 mM  $\text{Hg}^{2+}$  was added (Fig. 1). Upon addition of 1 mM  $\text{Hg}^{2+}$  to the mixture solution, its color rapidly changed from red to blue (existing in insert of the Fig. 1).  $\text{Hg}^{2+}$  was combined with papain and PDCA, decreased the distance of AuNPs, which result a shift of the surface plasma resonance peak and red-to-blue color changes. The UV-Vis absorption spectra of this sensor system became broader and shifted to much longer wavelength (650 nm). Transmission electron microscope (TEM) images of functionalized AuNPs (Fig. 2) also proved the aggregation of P-PDCA-AuNPs. The results proved that the papain and PDCA were sensitively responded to  $\text{Hg}^{2+}$ .

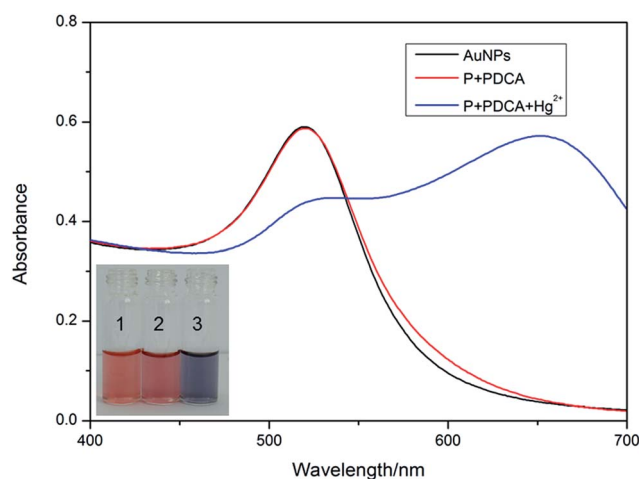


Fig. 1 UV-Vis absorption spectra of the AuNPs (13 nm), P-PDCA-AuNPs (13 nm), and P-PDCA-AuNPs (13 nm) in the presence of 1 mM of  $\text{Hg}^{2+}$ . Inset shows the color change versus the (1) AuNPs (13 nm), (2) P-PDCA-AuNPs (13 nm), and (3) P-PDCA-AuNPs (13 nm) in the presence of 1 mM of  $\text{Hg}^{2+}$ .

### 3.2. Optimal of papain concentration

To obtain the optimum concentration of the sensor system, we studied the effect of papain concentration on the stability of this system. To get excellent sensitivity, we obtained the AuNPs solutions at pH 6.0 and 30 °C. Concentrations of  $1.0 \times 10^{-5}$ ,  $1.0 \times 10^{-6}$ ,  $1.0 \times 10^{-7}$ ,  $1.0 \times 10^{-8}$  M papain were added to 2.12 nM AuNPs solutions. In order to make the PDCA combine with AuNPs closely, excessive amount of PDCA ( $5.0 \times 10^{-4}$  M) was added to the solutions. When PDCA and papain were added to the solution, the color of AuNPs had a little change. After adding 1 mM  $\text{Hg}^{2+}$ , the color became purple gradually along with the increase of concentration in 15 min (Fig. S-3 and insert of Fig. S-1†). With the decrease of the concentration, the absorbance of P-PDCA-AuNPs increases gradually at 520 nm and correspondingly decreases at 650 nm. But it is opposite to the concentration of  $1.0 \times 10^{-8}$  M. We use the ratio of the absorbance of P-PDCA-AuNPs at 650 and 520 nm ( $A_{650}/A_{520}$ ) to prove the degree of AuNPs aggregation (Fig. S-2†). A higher  $A_{650}/A_{520}$  value is bound up with the degree of AuNPs aggregation, and a lower  $A_{650}/A_{520}$  indicates that the AuNPs disperse well in the solution. When the concentration of papain is  $1.0 \times 10^{-7}$  M, the value of  $A_{650}/A_{520}$  comes to the highest, which indicates that the aggregation of P-PDCA-AuNPs is completely. Taking into account the response sensitivity and background signal,  $1.0 \times 10^{-7}$  M papain was selected as the optimized concentration.

### 3.3. Temperature and pH effects to functionalized AuNPs

Temperature and pH are two crucial factors of the sensitivity in this research. In order to investigate the pH effect of colorimetric responses, different pH (6, 7, 8 and 9) of functionalized AuNPs was obtained. Firstly, the pH of AuNPs solution (0.2 mL) was adjusted to 6, 7, 8 and 9, respectively, then 0.2 mL papain and PDCA were added. The P-PDCA-AuNPs was easily aggregated at acid aqueous solutions ( $\text{pH} \leq 6.0$ ). When the pH was high ( $\geq 6.0$ ), the P-PDCA-AuNPs were stable.<sup>35,40</sup> With the increase of pH values, the P-PDCA-AuNPs were more stable, which was possibly attributed that the electrostatic repulsion between the detection systems increased with the pH value.<sup>35</sup> Thus, in the presence of  $\text{Hg}^{2+}$ , the detection solutions exhibited obvious color change and the P-PDCA-AuNPs were easily induced aggregation at pH 6. The ratio value of  $A_{620}/A_{520}$  at pH 6 was also much greater than that at pH 7, 8, and 9 (Fig. S-4†), which demonstrated the pH of 6 was the optimal pH for this

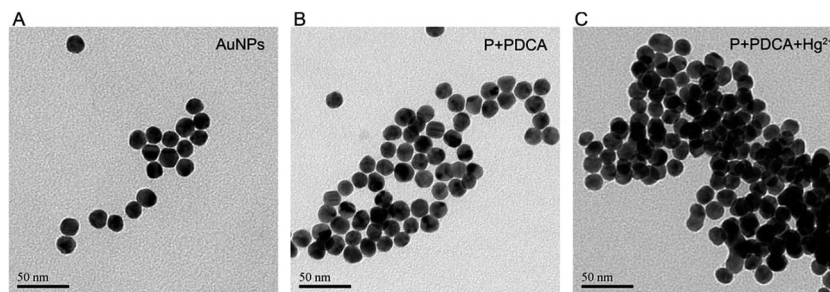


Fig. 2 TEM images of the (A) AuNPs (13 nm), (B) P-PDCA-AuNPs (13 nm) and (C) P-PDCA-AuNPs (13 nm) in the presence of 1 mM of  $\text{Hg}^{2+}$ .



sensor system. Hence, we chose the pH 6 as the optimal condition in this work. In order to demonstrate the temperature effect of functionalized AuNPs on the detection of  $\text{Hg}^{2+}$ , nine different temperatures (10, 20, 30, 40, 50, 60, 70, 80, 90 °C) of P-PDCA-AuNPs were obtained through setting the AuNPs solutions to the refrigerator and water bath, respectively. Then 0.2 mL  $\text{Hg}^{2+}$  (1 mM) were added. After incubation 15 min, the absorbance at 650 nm of the solutions was measured on a UV-2700 (Shimadzu) spectrophotometer. The ratio of absorbance of the UV-Vis absorption spectra at 650 and 520 nm ( $A_{650}/A_{520}$ ) was used to demonstrate the amount of functionalized AuNPs aggregation (Fig. S-5†). In the addition of  $\text{Hg}^{2+}$  (1 mM), with the increase of temperature to 30 °C, the ratio of  $A_{650}/A_{520}$  increased too, then it declined very slowly. When it reached 90 °C, the ratio of  $A_{650}/A_{520}$  decreased sharply. That is because papain has highly sensitivity temperature stability and starts losing its activation at 90 °C.<sup>41,42</sup> Results showed that the best temperature was range from 30 °C to 60 °C. Therefore, 30 °C was selected as the optimal temperature in this work. As a result, the P-PDCA-AuNPs sensor could be used as a colorimetric sensor for  $\text{Hg}^{2+}$  in a broad temperature range, which is convenient for a practical application.

### 3.4. Colorimetric detection of $\text{Hg}^{2+}$

It is well known that  $\text{Hg}^{2+}$  tends to interact with carboxylic group and amino such as PDCA<sup>19,47,48</sup> and cysteine.<sup>49</sup> Thus, a rational strategy to determine  $\text{Hg}^{2+}$  is to combine P-PDCA-AuNPs and  $\text{Hg}^{2+}$ . Inspired by this theory and under the best optimized detection condition (pH 6.0 for 15 min at 30 °C), the different concentrations of  $\text{Hg}^{2+}$  were added to P-PDCA-AuNPs to investigate the sensitivity of this sensor. As shown in Fig. 3A, with the increase of  $\text{Hg}^{2+}$  concentration, a decrease in the intensity of the absorbance at 520 nm and an increase at 650 nm can be observed. It revealed that the P-PDCA-AuNPs aggregation induced deposition with the rising of  $\text{Hg}^{2+}$  concentration. As envisioned, when different amounts of  $\text{Hg}^{2+}$  were added to an aqueous solution of P-PDCA-AuNPs, the color change of the solution (from red to blue) was observed by naked eye inspection (Fig. 3B). The lowest detection concentration with the unaided eye is 2  $\mu\text{M}$ . The ratio of  $A_{650}/A_{520}$  as a function of the concentration of  $\text{Hg}^{2+}$  is shown in Fig. 4, which increases gradually with the rise of the concentration of  $\text{Hg}^{2+}$ . A linear correlation exists in insert of the Fig. 4. Under the optimum conditions, the detection of  $\text{Hg}^{2+}$  was linear with  $A_{650}/A_{520}$  values in the range of 0.01  $\mu\text{M}$  to 14  $\mu\text{M}$ . The calibration equation was obtained by fitting the experimental data obtained:

$$y = (0.0252 \pm 0.0002)x + (0.1139 \pm 0.0005)$$

where  $y$  was the ratio of spectral absorbance  $A_{650}/A_{520}$ , and  $x$  was the concentration of  $\text{Hg}^{2+}$  ( $\mu\text{M}$ ). Additionally, the correlation coefficient of this equation was 0.9959. The sensor exhibited a detection limit of 9 nM (1.8 ppb), which met the MAL (maximum allowable level) of  $\sim 2$  ppb in drinking water set by the Environmental Protection Agency (EPA). In the presence of high concentration of  $\text{Hg}^{2+}$ , the UV-Vis absorption spectra

became broader and showed red shift and the  $A_{650}/A_{520}$  value was not in a linear range. Compared with other sensors (Table 1), the sensitivity of this method was also impressive.

### 3.5. Selectivity and interference study

The results above indicate that the P-PDCA-AuNPs sensor is sensitive to the determination of  $\text{Hg}^{2+}$ . As a functional sensor system, there must be high selectivity for  $\text{Hg}^{2+}$  over other ions. A

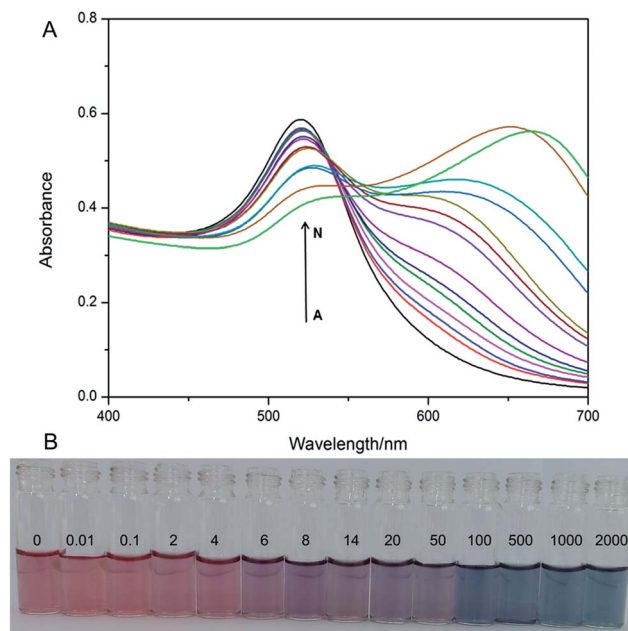


Fig. 3 (A) UV-Vis absorption spectra of P-PDCA-AuNPs were in the presence of different concentrations of  $\text{Hg}^{2+}$  (A to N express 2000, 1000, 500, 100, 50, 20, 14, 8, 6, 4, 2, 0.1, 0.01, 0  $\mu\text{M}$ , respectively). (B) Images of P-PDCA-AuNPs containing different concentrations of  $\text{Hg}^{2+}$  (0, 0.01, 0.1, 2, 4, 6, 8, 14, 20, 50, 100, 500, 1000, 2000  $\mu\text{M}$ ).

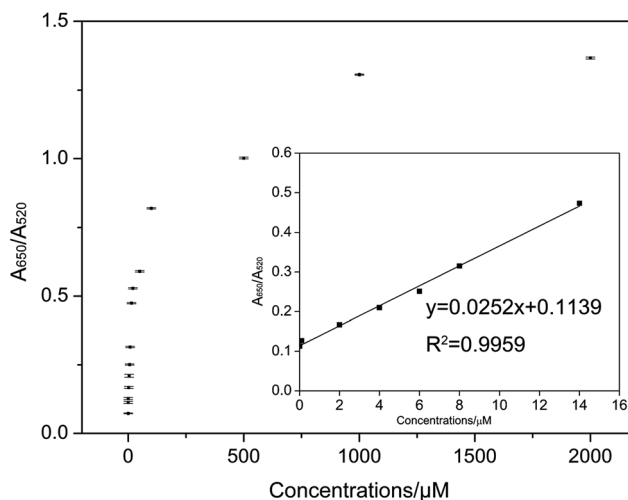


Fig. 4 Ratio values of  $A_{650}/A_{520}$  for P-PDCA-AuNPs versus the concentrations of  $\text{Hg}^{2+}$  (0, 0.01, 0.1, 2, 4, 6, 8, 14, 20, 50, 100, 500, 1000, 2000  $\mu\text{M}$ ). Image of insert is the linear correlation. Error bars were obtained from three experiments.

**Table 1** Functionalized AuNPs probes for detection of  $\text{Hg}^{2+}$ 

Technique	Capping agent	LOD (nM)	Linear range ( $\mu\text{M}$ )	Reference
Fluorescence	<sup>a</sup> BSA, R6G and MPA	10	Not given	Chang <i>et al.</i> <sup>50</sup>
	<sup>b</sup> RB and PDCA	10	0.015–0.25	Huang and Chang <sup>47</sup>
<sup>§</sup> FRET	<sup>c</sup> NAC-QDs and R6G	249	24.9–124.6	Hu <i>et al.</i> <sup>51</sup>
	RB6, MPA and <sup>d</sup> AMP	50	0.05–1.0	Yu and Tseng <sup>52</sup>
Colorimetry	<sup>e</sup> DNA (MSD)	30	0.02–1.0	Tan <i>et al.</i> <sup>53</sup>
	<sup>f</sup> CEQC	40	3.0–24	You <i>et al.</i> <sup>49</sup>
	Papain	4000	Not given	Guo <i>et al.</i> <sup>35</sup>
	DNA	1000	Not given	Xue <i>et al.</i> <sup>23</sup>
	DNA oligonucleotides	500	0–5	Xu <i>et al.</i> <sup>54</sup>
	MPA and AMP	500	0.5–3.5	Yu and Tseng <sup>52</sup>
	Thrombin-binding aptamer, PDCA	200	0.39–8.89	Wang <i>et al.</i> <sup>55</sup>
	Papain and PDCA	9	0.01–14	This work

<sup>a</sup> BSA, bovine serum albumin. R6G, rhodamine 6G. MPA, 3-mercaptopropionate acid. <sup>b</sup> RB, rhodamine B. <sup>c</sup> NAC-QDs, *N*-acetyl-L-cysteine functionalized quantum dots. <sup>d</sup> AMP, adenosine monophosphate. <sup>e</sup> MSD, 5'-SH(CH<sub>2</sub>)<sub>6</sub>A<sub>10</sub>TTCTTCTTCCCCTTGTGTGTT-FAM-3'. <sup>f</sup> CEQC, carboxylethyl quaternized cellulose. <sup>§</sup> FRET, fluorescence resonance energy transfer.

variety of competitive ions, including  $\text{Al}^{3+}$ ,  $\text{Ca}^{2+}$ ,  $\text{Cd}^{2+}$ ,  $\text{Cu}^{2+}$ ,  $\text{Fe}^{2+}$ ,  $\text{Fe}^{3+}$ ,  $\text{K}^+$ ,  $\text{Mg}^{2+}$ ,  $\text{Mn}^{2+}$ ,  $\text{NH}_4^+$ ,  $\text{Pb}^{2+}$ ,  $\text{Zn}^{2+}$  and  $\text{Na}^+$  ions, were added to the sensing system, the ratios of  $A_{650}/A_{520}$  were calculated. When only papain was functionalized on the surface of AuNPs, several commonly ions were tested using the papain-AuNPs (P-AuNPs) system. The assay showed negligible responses toward  $\text{Al}^{3+}$ ,  $\text{Ca}^{2+}$ ,  $\text{Cd}^{2+}$ ,  $\text{Fe}^{2+}$ ,  $\text{Fe}^{3+}$ ,  $\text{K}^+$ ,  $\text{Mg}^{2+}$ ,  $\text{Mn}^{2+}$ ,  $\text{NH}_4^+$ ,  $\text{Zn}^{2+}$  and  $\text{Na}^+$ , but a red-to-blue color change and red shift in the plasmon band energy to longer wavelengths were noted in the presence of  $\text{Hg}^{2+}$ ,  $\text{Cu}^{2+}$  as well as  $\text{Pb}^{2+}$ . It agreed with the findings of Guo *et al.*<sup>35</sup> Further higher selectivity of our sensor toward  $\text{Hg}^{2+}$  was achieved by adding PDCA. As shown in Fig. 5, except for  $\text{Hg}^{2+}$ , none of these competitive ions can induce the apparent aggregation of P-PDCA-AuNPs. Even though the concentrations of these ions were 20 times higher than that of  $\text{Hg}^{2+}$ , these ions induced negligible changes in comparison with  $\text{Hg}^{2+}$ . When all the other competitive ions were present in

a water sample solely, the P-PDCA-AuNPs solutions showed no obvious response. In contrast, when  $\text{Hg}^{2+}$  existed in the sample, the P-PDCA-AuNPs solutions aggregated and exhibited apparent color change simultaneously. Aggregation in the presence of  $\text{Hg}^{2+}$  is because of binding with chelating ligands, inducing both shift in the plasmon band energy to longer wavelength and a red-to-blue color change (Fig. S-6B†). In particular, PDCA ligands bound to the functionalized AuNPs system through Au–N bonds can improve the selectivity toward  $\text{Hg}^{2+}$  via a cooperative effect.<sup>19,36</sup>  $\text{Hg}^{2+}$  can cause the aggregation of P-PDCA-AuNPs with the obvious increase of  $A_{650}/A_{520}$  value. The plasma absorbance peak of  $\text{Hg}^{2+}$  has apparent red shift (Fig. S-6A†). Further,  $\text{Hg}^{2+}$  and other ions were mixed to form a mixture solution as a sample for the interference study of the sensor. The  $A_{650}/A_{520}$  value was obviously higher than other samples without  $\text{Hg}^{2+}$ . The results indicated that this sensor system could be utilized to detect  $\text{Hg}^{2+}$  with high selectivity. The selectivity in the presence of only PDCA was also developed, the results exhibited the selectivity was still not satisfactory. From all the results, it is concluded that functionalized of AuNPs surface with papain and PDCA is very important to increase the selectivity of  $\text{Hg}^{2+}$ . The PDCA ligands bound to the AuNPs species improved selectivity toward  $\text{Hg}^{2+}$  through the cooperative effect, while it formed complexes with other ions in the bulk solutions, suppressing their interference with the sensors. Moreover, in Fig. S-6B,† a purple-to-red color change can be observed in the presence of  $\text{Fe}^{2+}$ . That is because the PDCA ligands in the solution form complexes with  $\text{Fe}^{2+}$  and induce the shift in plasmon band energy to shorter wavelength.<sup>36</sup>

### 3.6. Analytical applications

To evaluate our sensor for the detection of  $\text{Hg}^{2+}$  in real samples, tap water samples from our laboratory, pond water from the Lake of Peach (Changsha, China) and river water samples from Hsiang River (Changsha, China) were used for this sensor. Firstly, we filtered the water samples through 0.22  $\mu\text{m}$  membrane. Then, river water, tap water and pond water were

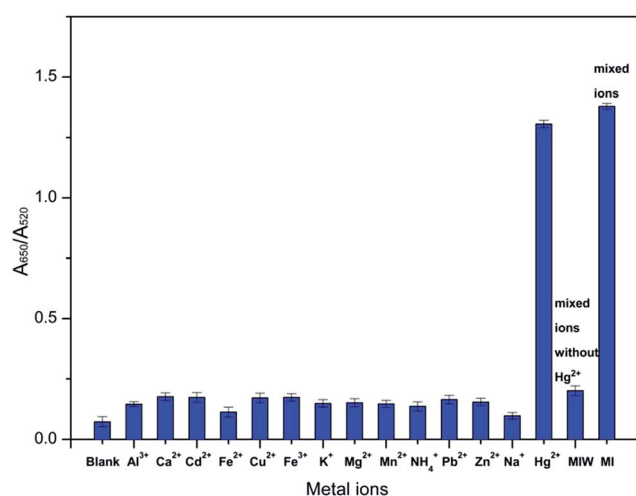


**Fig. 5** Ratio values of  $A_{650}/A_{520}$  for P-PDCA-AuNPs versus the different kinds of ions. Concentration of  $\text{Hg}^{2+}$  was 1 mM, while others were 20 mM. Error bars were obtained from three experiments.

**Table 2** Levels of  $\text{Hg}^{2+}$  in real samples were measured using our method and AFS measurement with the range of relative standard deviation from 0.10% to 2.52%

Samples	Added ( $\mu\text{M}$ )	Found ( $\mu\text{M}$ )	Recovery (%)	RSD <sup>a</sup> (%)	AFS <sup>b</sup>
Tap water	0.01	0.012	112.00	0.17	0.014
	5	5.03	100.60	1.00	5.13
	10	10.07	100.70	1.53	10.21
River water	0.01	0.013	113.00	0.15	0.016
	5	5.14	102.80	2.08	5.20
	10	10.27	102.70	2.00	10.40
Pond water	0.01	0.011	110.00	0.10	0.013
	5	5.10	102.00	1.75	5.15
	10	10.16	101.60	2.06	10.23

<sup>a</sup> RSD, relative standard deviation. <sup>b</sup> AFS, atomic fluorescence spectrometry.

spiked with standard  $\text{Hg}^{2+}$  solutions (0.01  $\mu\text{M}$ , 5  $\mu\text{M}$  and 10  $\mu\text{M}$ , respectively). The results were summarized in Table 2. As can be observed in Table 2, the recoveries of standard addition were between 0.01  $\mu\text{M}$  and 10  $\mu\text{M}$ . The data were then compared by the AFS measurement. The concentrations of  $\text{Hg}^{2+}$  in the spiked water samples detected by the P-PDCA-AuNPs sensor system with an external calibration revealed good agreement with those, which was determined with a standard addition calibration. It confirmed that there was no interference encountered in the analysis of these water samples.

## 4. Conclusions

In conclusion, we describe here a fast, sensitive and selective colorimetric detection of  $\text{Hg}^{2+}$  based on the principle that  $\text{Hg}^{2+}$  can induce the aggregation of the P-PDCA-AuNPs. The color of the P-PDCA-AuNPs solutions change from red to blue when different concentrations of  $\text{Hg}^{2+}$  ions were added, which can be monitored by UV-Vis spectra for the detection of  $\text{Hg}^{2+}$  in river water, tap water and pond water samples. Different kinds of ions make this detection system show good selectivity to  $\text{Hg}^{2+}$ . Under the optimum conditions (2.23 nM P-PDCA-AuNPs, 15 min, 30 °C to pH 6.0), the detection limit of this system was 9 nM (1.8 ppb), which is lower than the maximum allowable level of ~10 nM (2 ppb) in drinking water in the USA. The linear range of this sensor was 0.01  $\mu\text{M}$  to 14  $\mu\text{M}$  with a correlation coefficient of 0.9959. The sensor system herein presented has demonstrated to be sensitive and selective for the detection of  $\text{Hg}^{2+}$ . For its sensitivity and selectivity, we believe the detection system will have potential application in the development for monitoring  $\text{Hg}^{2+}$  in environmental samples. The results demonstrate fundamental understanding of the enzyme biochemistry, and it can lead to dramatically improved colorimetric sensors.

## Acknowledgements

We would like to thank the Program for the National Natural Science Foundation of China (51378190, 51278176, 51408206,

51579098, 51521006), the Fundamental Research Funds for the Central Universities, Hunan University Fund for Multidisciplinary Developing (531107040762), the Program for New Century Excellent Talents in University (NCET-13-0186), the Program for Changjiang Scholars and Innovative Research Team in University (IRT-13R17), Scientific Research Fund of Hunan Provincial Education Department (No. 521293050) support of this study.

## References

- 1 W.-W. Tang, G.-M. Zeng, J.-L. Gong, J. Liang, P. Xu, C. Zhang and B.-B. Huang, *Sci. Total Environ.*, 2014, **468**, 1014–1027.
- 2 P. Xu, G. M. Zeng, D. L. Huang, C. L. Feng, S. Hu, M. H. Zhao, C. Lai, Z. Wei, C. Huang and G. X. Xie, *Sci. Total Environ.*, 2012, **424**, 1–10.
- 3 C. Zhang, G. Zeng, D. Huang, C. Lai, C. Huang, N. Li, P. Xu, M. Cheng, Y. Zhou and W. Tang, *RSC Adv.*, 2014, **4**, 55511–55518.
- 4 L. Campbell, D. Dixon and R. Hecky, *J. Toxicol. Environ. Health, Part B*, 2003, **6**, 325–356.
- 5 T. J. Dickerson, N. N. Reed, J. J. LaClair and K. D. Janda, *J. Am. Chem. Soc.*, 2004, **126**, 16582–16586.
- 6 G. Zeng, M. Chen and Z. Zeng, *Science*, 2013, **340**, 1403.
- 7 C. J. Watras and J. W. Huckabee, *Mercury pollution integration and synthesis*, CRC Press, 1994.
- 8 G. Zeng, M. Chen and Z. Zeng, *Nature*, 2013, **499**, 154.
- 9 R. K. Zalups, *Pharmacol. Rev.*, 2000, **52**, 113–144.
- 10 T. W. Clarkson, L. Magos and G. J. Myers, *N. Engl. J. Med.*, 2003, **349**, 1731–1737.
- 11 V. N. Mehta and S. K. Kailasa, *RSC Adv.*, 2015, **5**, 4245–4255.
- 12 Y. Xiang, A. Tong and Y. Lu, *J. Am. Chem. Soc.*, 2009, **131**, 15352–15357.
- 13 M. Ravichandran, *Chemosphere*, 2004, **55**, 319–331.
- 14 R. Suddendorf, J. Watts and K. Boyer, *J. - Assoc. Off. Anal. Chem.*, 1981, **64**, 1105–1110.
- 15 C. M. Welch and R. G. Compton, *Anal. Bioanal. Chem.*, 2006, **384**, 601–619.
- 16 C.-C. Huang, Z. Yang, K.-H. Lee and H.-T. Chang, *Angew. Chem.*, 2007, **119**, 6948–6952.
- 17 A. Chatterjee, M. Santra, N. Won, S. Kim, J. K. Kim, S. B. Kim and K. H. Ahn, *J. Am. Chem. Soc.*, 2009, **131**, 2040–2041.
- 18 J. S. Lee, M. S. Han and C. A. Mirkin, *Angew. Chem., Int. Ed. Engl.*, 2007, **46**, 4093–4096.
- 19 D. Li, A. Wieckowska and I. Willner, *Angew. Chem., Int. Ed. Engl.*, 2008, **47**, 3927–3931.
- 20 Z. Chen, C. Zhang, H. Ma, T. Zhou, B. Jiang, M. Chen and X. Chen, *Talanta*, 2015, **134**, 603–606.
- 21 L. Cui, Z. Guang-Ming, D.-L. Huang, F. Chong-Ling, H. Shuang, S. Feng-Feng, Z. Mei-Hua, C. Huang and W. Zhen, *Chin. J. Anal. Chem.*, 2010, **38**, 909–914.
- 22 J.-L. Gong, B. Wang, G.-M. Zeng, C.-P. Yang, C.-G. Niu, Q.-Y. Niu, W.-J. Zhou and Y. Liang, *J. Hazard. Mater.*, 2009, **164**, 1517–1522.
- 23 X. Xue, F. Wang and X. Liu, *J. Am. Chem. Soc.*, 2008, **130**, 3244–3245.
- 24 Z. Wang and L. Ma, *Coord. Chem. Rev.*, 2009, **253**, 1607–1618.

- 25 S. S. Agasti, S. Rana, M. H. Park, C. K. Kim, C. C. You and V. M. Rotello, *Adv. Drug Delivery Rev.*, 2010, **62**, 316–328.
- 26 C. Zhang, L. Liu, G.-M. Zeng, D.-L. Huang, C. Lai, C. Huang, Z. Wei, N.-J. Li, P. Xu and M. Cheng, *Biochem. Eng. J.*, 2014, **91**, 149–156.
- 27 A. Baghel, B. Singh, P. Pandey and K. Sekhar, *Anal. Sci.*, 2007, **23**, 135–137.
- 28 Y. M. Guo, Y. Zhang, H. W. Shao, Z. Wang, X. F. Wang and X. Y. Jiang, *Anal. Chem.*, 2014, **86**, 8530–8534.
- 29 H. N. Kim, W. X. Ren, J. S. Kim and J. Yoon, *Chem. Soc. Rev.*, 2012, **41**, 3210–3244.
- 30 Y. W. Lin, C. C. Huang and H. T. Chang, *Analyst*, 2011, **136**, 863–871.
- 31 J. Du, S. Yin, L. Jiang, B. Ma and X. Chen, *Chem. Commun.*, 2013, **49**, 4196–4198.
- 32 Y. G. Wu, L. Liu, S. S. Zhan, F. Z. Wang and P. Zhou, *Analyst*, 2012, **137**, 4171–4178.
- 33 Y. G. Wu, F. Z. Wang, S. S. Zhan, L. Liu, Y. F. Luo and P. Zhou, *RSC Adv.*, 2013, **3**, 25614–25619.
- 34 X. J. Xue, F. Wang and X. G. Liu, *J. Am. Chem. Soc.*, 2008, **130**, 3244–3245.
- 35 Y. Guo, Z. Wang, W. Qu, H. Shao and X. Jiang, *Biosens. Bioelectron.*, 2011, **26**, 4064–4069.
- 36 G. K. Darbha, A. K. Singh, U. S. Rai, E. Yu, H. Yu and P. Chandra Ray, *J. Am. Chem. Soc.*, 2008, **130**, 8038–8043.
- 37 C. J. Yu, T. L. Cheng and W. L. Tseng, *Biosens. Bioelectron.*, 2009, **25**, 204–210.
- 38 C. Lai, G.-M. Zeng, D.-L. Huang, M.-H. Zhao, Z. Wei, C. Huang, P. Xu, N.-J. Li, C. Zhang and M. Chen, *Spectrochim. Acta, Part A*, 2014, **132**, 369–374.
- 39 M. Kalita, S. Balivada, V. P. Swarup, C. Mencia, K. Raman, U. R. Desai, D. Troyer and B. Kuberan, *J. Am. Chem. Soc.*, 2014, **136**, 554–557.
- 40 I. B. Kim and U. H. F. Bunz, *J. Am. Chem. Soc.*, 2006, **128**, 2818–2819.
- 41 P. Kaul, H. Sathish and V. Prakash, *Food Nahrung*, 2002, **46**, 2–6.
- 42 X. Y. Liu, H. Y. Zeng, M. C. Liao, B. Feng and B. F. C. A. Gohi, *Biochem. Eng. J.*, 2015, **97**, 125–131.
- 43 C. Lai, G.-M. Zeng, D.-L. Huang, M.-H. Zhao, H.-L. Huang, C. Huang, Z. Wei, N.-J. Li, P. Xu and C. Zhang, *Int. Biodeterior. Biodegrad.*, 2013, **82**, 180–186.
- 44 J. R. Kalluri, T. Arbneshi, S. A. Khan, A. Neely, P. Candice, B. Varisli, M. Washington, S. McAfee, B. Robinson, S. Banerjee, A. K. Singh, D. Senapati and P. C. Ray, *Angew. Chem., Int. Ed.*, 2009, **48**, 9668–9671.
- 45 J. M. Slocik, M. O. Stone and R. R. Naik, *Small*, 2005, **1**, 1048–1052.
- 46 J. Xie, Y. Zheng and J. Y. Ying, *J. Am. Chem. Soc.*, 2009, **131**, 888–889.
- 47 C. C. Huang and H. T. Chang, *Anal. Chem.*, 2006, **78**, 8332–8338.
- 48 R. Dominguez-Gonzalez, L. G. Varela and P. Bermejo-Barrera, *Talanta*, 2014, **118**, 262–269.
- 49 J. You, H. Hu, J. Zhou, L. Zhang, Y. Zhang and T. Kondo, *Langmuir*, 2013, **29**, 5085–5092.
- 50 H. Y. Chang, T. M. Hsiung, Y. F. Huang and C. C. Huang, *Environ. Sci. Technol.*, 2011, **45**, 1534–1539.
- 51 B. Hu, L.-L. Hu, M.-L. Chen and J.-H. Wang, *Biosens. Bioelectron.*, 2013, **49**, 499–505.
- 52 C. J. Yu and W. L. Tseng, *Langmuir*, 2008, **24**, 12717–12722.
- 53 D. Tan, Y. He, X. Xing, Y. Zhao, H. Tang and D. Pang, *Talanta*, 2013, **113**, 26–30.
- 54 X. Xu, J. Wang, K. Jiao and X. Yang, *Biosens. Bioelectron.*, 2009, **24**, 3153–3158.
- 55 Y. Wang, F. Yang and X. Yang, *Biosens. Bioelectron.*, 2010, **25**, 1994–1998.